Creep Behavior of Glass-Fiber-Reinforced Nylon 6 Products

Hironori Tohmyoh,[1] Yusuke Ito,[1] Kazuteru Eguchi,[2] Wataru Daido,[2] Jiro Utsunomiya,[2] Yoshikatsu Nakano[3]

[1]*Department of Nanomechanics, Tohoku University, Aoba 6-6-01, Aramaki, Aoba-ku, Sendai 980-8579, Japan*
[2]*Keihin Corporation, Houshakuji 2021-8, Takanezawa, Shioya, Tochigi 329-1233, Japan*
[3]*Institute of Fluid Science, Tohoku University, Katahira 2-2-1, Aoba-ku, Sendai 980-8577, Japan*

Received 2 June 2011; accepted 30 July 2011
DOI 10.1002/app.35393
Published online 29 November 2011 in Wiley Online Library (wileyonlinelibrary.com).

ABSTRACT: The creep properties, that is, the velocity constant, activation energy, stress index, and time index, of a test piece (TP) cut from a glass-fiber-reinforced nylon 6 product were successfully determined by a compression creep test. In the determination of the creep properties, the experimental creep curves for the TP were fitted by finite element analysis (FEA). Fiber-reinforced nylon 6 beams with different fiber orientations were also prepared, and their creep properties were successfully determined by a combination of the bending creep test and the corresponding analysis. The creep behavior of the press-fit component composed of a metal collar and a fiber-reinforced nylon 6 product was predicted by FEA with the determined creep properties of the TP. The predicted retention forces were in good agreement with the experimental ones. The effects of the fiber orientation on the long-term reliability of the press-fit component are also discussed. © 2011 Wiley Periodicals, Inc. J Appl Polym Sci 124: 4213–4221, 2012

Key words: creep; fibers; injection molding; nylon; relaxation

INTRODUCTION

Fiber-reinforced polymer materials have many advantages, including their light weight and high strength, and have been widely used as structural materials in vehicles, for example, automobiles[1] and aircraft.[2] The use of fiber-reinforced polymer parts rather than metal parts for the structural material of a vehicle reduces its weight and, consequently, contributes to an improvement in fuel cost. Transport vehicles are used in various environments, and fiber-reinforced polymer material, which may be subjected to stress in a high-temperature environment over a long period of time, can suffer from creep deformation.[3,4] A knowledge of the creep deformation is important for ensuring the long-term reliability of fiber-reinforced polymer products.

However, the creep behavior of fiber-reinforced polymer products is usually difficult to predict because of its complexity. The creep properties of polymer materials are known to show time dependency[5,6] and are affected by aging time,[7,8] moisture content,[9,10] thickness,[11] and so on. Also, the physical properties of fiber-reinforced polymer materials are heavily dependent on the characteristics of the fibers,[12–14] such as fiber orientation,[13] fiber length[14] and so on. To understand or predict the complex viscoelastic properties of fiber-reinforced polymer materials, finite element analysis (FEA) based on micromechanics has been widely used.[15–17] Particularly, the FEA approach combined with a homogenization theory successfully represents the stress–strain fields of the polymer composites in the nonlinear state.[18] As described previously, because the creep properties of polymer materials show a complex nature, the creep properties of fiber-reinforced polymer materials obtained from a specimen may not be directly used in a creep analysis of the actual products, even if the creep properties are determined from a conventional creep test.

In this article, a procedure for predicting the creep behavior of fiber-reinforced polymer products by FEA is described. The test target was a press-fit component composed of a fiber-reinforced nylon 6 product and a metal collar. The metal collar was inserted into a hole in the fiber-reinforced nylon 6 product, and the press-fit component was subjected to high temperature. The contact pressure between the collar and the product decreased with time due to creep deformation. First, the creep properties, that is, the velocity constant, activation energy (ΔH), stress index (n), and time index (m), of the fiber-reinforced nylon 6 product were determined from a test piece (TP) cut from the product by the methodology

Correspondence to: H. Tohmyoh (tohmyoh@ism.mech.tohoku.ac.jp).

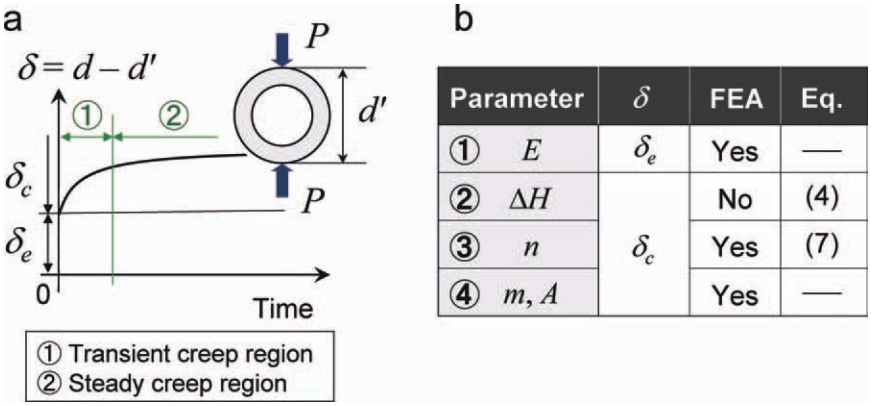

Figure 1 (a) Schematic of the constant load creep test and creep curve. (b) Details of the determination of the creep properties. [Color figure can be viewed in the online issue, which is available at wileyonlinelibrary.com.]

proposed in this article. The creep behavior of the press-fit component was simulated by FEA with the creep properties determined directly from the product. Moreover, with the creep properties determined from the fiber-reinforced nylon 6 beams with different fiber orientations, the effect of the fiber orientation on the long-term reliability of the press-fit component was analyzed and is discussed.

DETERMINATION OF THE CREEP PROPERTIES

It is well known that the creep deformation of a polymer material is time-dependent,[4–7] and the behavior can be described by the following equation[19,20]:

$$\frac{d\varepsilon_c}{dt} = A \exp\left(-\frac{\Delta H}{RT}\right)\sigma^n m t^{m-1} \tag{1}$$

where ε_c is the creep strain, t is the time, A is the velocity constant, R (=8.31447 J/mol) is the gas constant, T is the temperature, and σ is the stress. The four parameters A, ΔH, n, and m are material dependent and need to be determined to describe the creep character of the material.

Let us consider the constant-load creep test shown in Figure 1(a), where the cylindrical sample is at temperature T. The sample is subjected to a load (P) at its center. The diameters of the samples with and without load are indicated by d and d', respectively. The displacement at the loading point is given by $\delta = d - d'$. Figure 1(a) shows an example of a creep curve, that is, δ versus t for the fiber-reinforced polymer material. δ_e and δ_c indicate the elastic and creep displacements, respectively. Immediately after the load is applied, the sample deforms elastically, and δ_c is initiated. The creep speed ($d\varepsilon_c/dt$) is determined from the slope of the δ–t relationship. $d\varepsilon_c/dt$ decreases gradually with increasing time, and it approaches a constant value. The region with a constant value of $d\varepsilon_c/dt$ is called the *steady creep region*, and the region before the steady creep region with various $d\varepsilon_c/dt$ values is called the *transient creep region*. The creep properties of the fiber-reinforced nylon 6 material were derived from the δ–t relationship with the aid of FEA.

Figure 1(b) summarizes the details of the creep properties. First, the Young's modulus (E) was determined from the elastic region of the δ–t curve. Elastic FEA was performed repeatedly until the δ determined by FEA matched the δ_e obtained experimentally. From this, E could be determined.

To determine ΔH, we considered two experimental conditions performed under the same load and at different temperatures (T_1 and T_2). The values of $d\varepsilon_c/dt$ for T_1 and T_2 are given by

$$\left.\frac{d\varepsilon_c}{dt}\right|_{T=T_1} = A \exp\left(-\frac{\Delta H}{RT_1}\right)\sigma^n m t^{m-1} \tag{2}$$

and

$$\left.\frac{d\varepsilon_c}{dt}\right|_{T=T_2} = A \exp\left(-\frac{\Delta H}{RT_2}\right)\sigma^n m t^{m-1} \tag{3}$$

From eqs. (2) and (3), we get

$$\Delta H = \ln\left(\frac{d\varepsilon_c/dt|_{T=T_1}}{d\varepsilon_c/dt|_{T=T_2}}\right)\frac{T_1 T_2}{T_1 - T_2}R \tag{4}$$

To determine n, we considered two experimental conditions performed at the same temperature and under different loads, where the corresponding stresses were described as σ_1 and σ_2, respectively. The values of $d\varepsilon_c/dt$ for σ_1 and σ_2 are given by

$$\left.\frac{d\varepsilon_c}{dt}\right|_{\sigma=\sigma_1} = A \exp\left(-\frac{\Delta H}{RT}\right)\sigma_1^n m t^{m-1} \tag{5}$$

and

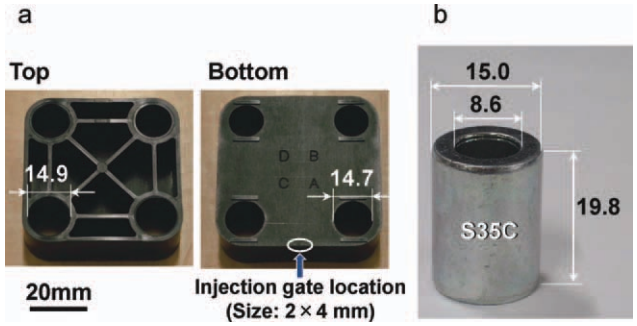

Figure 2 (a) Top and bottom views of the test product. The test product was made of nylon 6 and contained about 30 wt % glass fibers. (b) Metal collar. [Color figure can be viewed in the online issue, which is available at wileyonlinelibrary.com.]

$$\left.\frac{d\varepsilon_c}{dt}\right|_{\sigma=\sigma_2} = A\exp\left(-\frac{\Delta H}{RT}\right)\sigma_2^n m t^{m-1} \tag{6}$$

From eqs. (5) and (6), we get

$$n = \frac{\ln\left(d\varepsilon_c/dt|_{\sigma=\sigma_2}\right) - \ln\left(d\varepsilon_c/dt|_{\sigma=\sigma_1}\right)}{\ln\sigma_2 - \ln\sigma_1} \tag{7}$$

The values of σ_1 and σ_2 were determined by FEA, and the maximum values of the equivalent von Mises stress working at the loading point on the sample were used for σ_1 and σ_2 in this study.

The parameter m represents the time dependency of the material, and the information appears at an early stage in the creep behavior, that is, at the transient creep region. As shown in Figure 1(a), ε_c rapidly increased with time and then reached a steady state. A smaller m gave a shorter period before the steady state was reached. On the other hand, the material required a longer time to reach the steady creep state when the material had a large m. The value of m, therefore, could be determined from the creep transition time, that is, the time required before the steady creep state was reached. However, because the steady creep behavior and the transient creep behavior were dependent on m, m and A needed to be resolved together, as described in the following paragraph.

The remaining parameter, A, which affects the speed in the steady creep state, was determined by FEA. First, we determined $d\varepsilon_c/dt$ in the steady creep region with FEA by the assumption of A ($d\varepsilon_c/dt\,|_{\mathrm{FEA}}$). A was determined from

$$A = \frac{d\varepsilon_c/dt|_{EXP}}{d\varepsilon_c/dt|_{FEA}} A_{FEA} \tag{8}$$

where $d\varepsilon_c/dt\,|_{\mathrm{EXP}}$ is obtained from the experiment. All of the creep parameters, A, ΔH, n, and m, could now be successfully determined by the previous steps.

EXPERIMENTAL PROCEDURE AND NUMERICAL ANALYSIS

TP and creep test

Figure 2(a) shows photographs of the top and bottom of a fiber-reinforced nylon 6 product made from a thermoplastic resin (CM1016G-30, Toray Industries, Inc., Tokyo, Japan) by an injection-molding machine for this study. The holes were partly fixed by rigid supports. The resin material was nylon 6 containing about 30 wt % glass fibers. The hole had a tapered structure with the larger diameter at the top. The inner diameters of the hole were 14.9 mm (top) and 14.7 mm (bottom), and the height was 20.1 mm. The metal collar, which was inserted from the top side, was made of S35C. The outer and inner diameters of the collar were 15.0 and 8.6 mm, respectively [Fig. 2(b)].

Figure 3(a) shows an overall view of the creep test apparatus used in this study. To determine the creep properties of the test product, a cylindrical sample was cut from it [Fig. 3(b)]. The thickness of the sample was 3 mm, and the thickness of the wall was 1 mm. The cylindrical sample was set in the creep test apparatus, where it was subjected to a constant compressive load by a wire–pulley–weight system, and the displacement–time relationships under three combinations of two loads and two temperatures were obtained. When a weight was hung on the wire, a load was applied to the center of the test product through the pulley. In the creep test, the test apparatus was placed in a temperature-controlled chamber. The displacement at the loading point was measured at plane B in Figure 3(b) by a laser displacement sensor through a window in the chamber. Creep tests were performed at temperatures of 343 and 393 K.

To investigate the effect of fiber orientation on the creep properties of the fiber-reinforced nylon 6

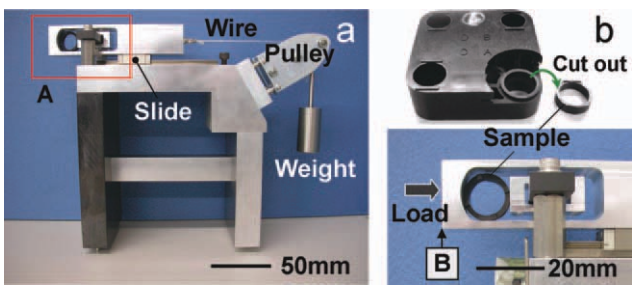

Figure 3 (a) Overall view of the creep test apparatus. (b) Details of A in (a). Here, the displacement at a point on plane B was measured by a laser displacement sensor. [Color figure can be viewed in the online issue, which is available at wileyonline library.com.]

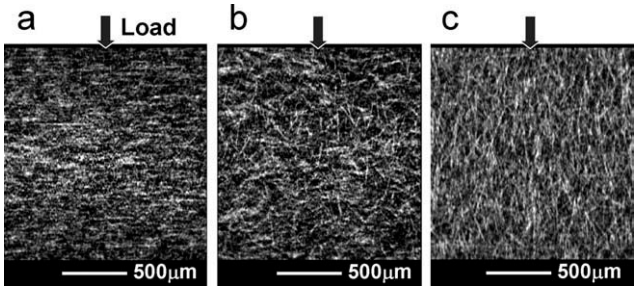

Figure 4 Computed tomography images of the (a) FV, (b) FR, and (c) FP samples. The arrow indicates the direction of the applied load in the three-point-bending creep test.

product, three types of beam samples with different fiber orientations in the nylon 6 were prepared. The length and cross sectional area of the beam samples were 100 mm and 5×3 mm^2, respectively, and the sample contained about 30 wt % glass fibers. In this study, three-point-bending creep tests were adopted. The loading system of the creep test apparatus was changed for bending tests. Here, both ends of the beam sample were simply supported, and the load was applied at the center. The beam sample was supported by two fulcrums, the distance between which was 87.2 mm. Creep tests were performed at temperatures of 343 and 393 K. Figure 4 shows computed tomography images of the test samples obtained around the loading point. The direction of the load for three-point bending is indicated by arrows in the figures. From the figures, we found that each sample had a different fiber orientation. The beam sample with fibers arranged in a vertical direction with respect to the load was called the FV sample [Fig. 4(a)]. The beam sample with fibers arranged randomly was called the FR sample [Fig. 4(b)], and the beam sample with fibers arranged in a perpendicular direction with respect to the load was called the FP sample [Fig. 4(c)]. We also prepared a nylon 6 sample without fibers.

Stress relaxation test

The details of the stress relaxation test are shown in Figure 5. The collar was inserted into the hole with a universal test machine with a crosshead speed of 10 mm/min, and the load–displacement relationship was recorded [Fig. 5(a)]. The press-fit component was placed in a temperature-controlled chamber at 343 or 393 K for 2, 6, or 24 h. After 24 h, the product was removed from the chamber and cooled down to room temperature. Finally, pullout tests were performed [Fig. 5(b)]. The test machine and the crosshead speed for the pullout tests were the same as those used for insertion of the metal collar. The maximum force recorded during the pullout tests was defined as the *retention force*, and we measured the values of this for each temperature condition.

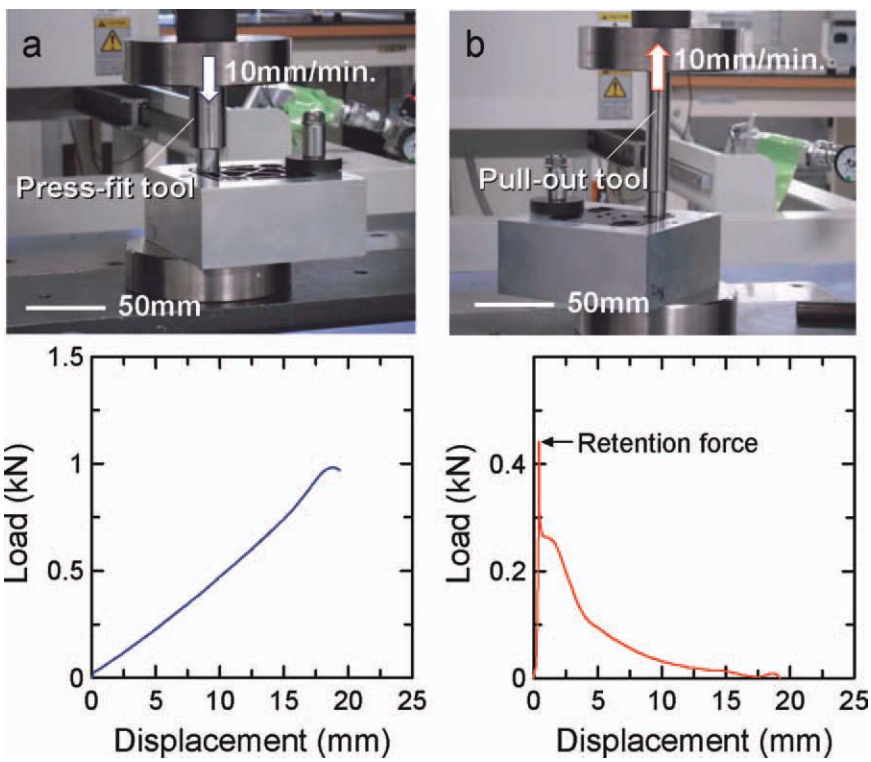

Figure 5 Stress relaxation test: (a) insertion of the metal collar into the hole in the test product and (b) the pulling of the collar out of the hole. [Color figure can be viewed in the online issue, which is available at wileyonlinelibrary.com.]

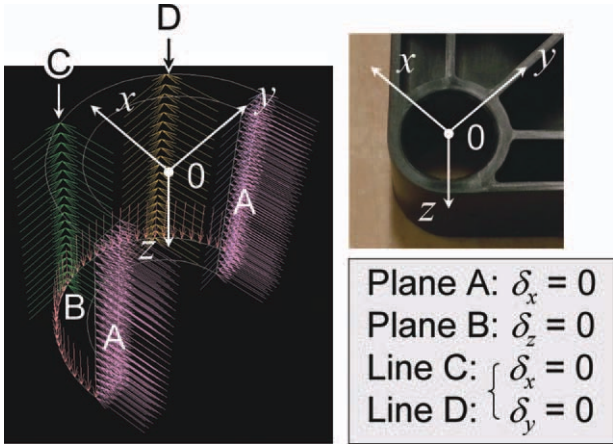

Figure 6 FE model used in this study. [Color figure can be viewed in the online issue, which is available at wileyonlinelibrary.com.]

Numerical analysis

The nonlinear structural analysis software MARC (MSC Software Corp., Santa Ana, CA) was used to determine the creep properties of the TP cut from the fiber-reinforced nylon 6 product. Before the creep analysis, it was necessary to determine E. This was done with FEA to find the central displacement of the cylindrical sample that corresponded with the initial displacement of the sample before the creep deformation was experimentally obtained. With this value of E, we performed creep analysis using the procedure described in the previous section.

Figure 6 shows the finite element (FE) model used in the stress relaxation analysis of the press-fit component. In the analysis, a ½ model was employed. Because E of the metal collar was much higher than that of the fiber-reinforced nylon 6 product, the collar was assumed to be a rigid body. The creep properties of the cylindrical sample cut from the test product were used. As discussed in the next section, the creep properties of the fiber-reinforced nylon 6 material showed anisotropy. Here, the creep properties of the cylindrical sample were determined for the radial direction loading by a compression test. Also, the press-fit component was suffered from the radial direction loading by the insertion of the metal collar, and the loading directions of both cases were in agreement with each other. Therefore, press-fit analysis for the real product could be done with the determined creep properties of the cylindrical sample. The radial force acting on the metal collar (F) was determined in this study. The retention force was given by

$$P = \mu F \tag{9}$$

where μ is the coefficient of friction between the metal collar and the resin product. Therefore, the time- and temperature-dependent behaviors of F were in agreement with P, provided that μ was constant. We determined the reaction force in the x direction (F_x) acting on the metal collar by FEA under no-friction conditions,[21] and F was then determined from the following equation:

$$F = \frac{2\pi F_x}{\int_0^\pi \sin\theta d\theta} \tag{10}$$

where θ is the angle between the x axis and the radial direction on the surface of the metal collar. In the analysis, Poisson's ratio for all components was assumed to be 0.3.

EXPERIMENTAL RESULTS AND DISCUSSION

Creep properties

Figure 7(a) shows the relationships between the displacement and the time obtained from the compressive creep test of the cylindrical sample under three combinations of temperature and load, together with

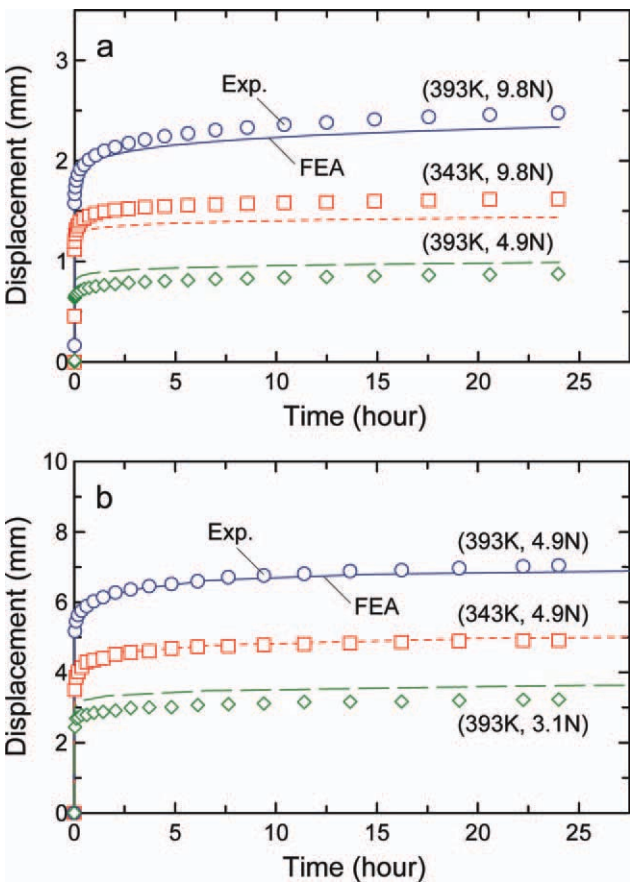

Figure 7 (a) Creep curves for the TP sample obtained from the experiment (plot) and from FEA (curve) after fitting. (b) Examples of the creep curves for the FP sample together with the corresponding results of FEA after fitting. [Color figure can be viewed in the online issue, which is available at wileyonlinelibrary.com.]

TABLE I
Creep Properties of the TP Cut from the Product

Sample	A (Pa^{-n} s^{-m})	n	ΔH (kJ/mol)	m
TP	1.27×10^{-12}	1.72	25.1	0.1

the corresponding results of FEA after nonlinear fitting. The nonlinear fitting of FEA with the experimental results was performed with the procedure described in this article. The FEA results were in reasonable agreement with the experimental ones. This suggested that the creep properties of the TP were determined successfully. The creep properties of the TP are summarized in Table I.

Figure 7(b) shows examples of the creep test curves, that is, displacement versus time, for the FP sample, together with the corresponding results of FEA after fitting. For all of the combinations of temperature and load, the creep curves obtained by FEA were in reasonable agreement with the experimental ones. Similar agreement between the experimental creep curves and FEA were found for the FV and FR samples. This suggested that the nonlinear fitting of the FEA was done successfully and that the creep properties of the beam samples were accurately determined.

The creep properties of the FV, FR, FP, and polymer samples are summarized in Table II. The data are also displayed in Figure 8. Of the examined samples, n of the FP sample had the highest value; this indicated that it had the highest stress dependency in the examined beam samples. On the other hand, the values of ΔH, which is an indicator of the temperature dependency of creep, were almost the same for all of the fiber-reinforced nylon 6 beams;

TABLE II
Creep Properties of the Beam Samples with Different Fiber Orientations

Sample	A (Pa^{-n} s^{-m})	n	ΔH (kJ/mol)	m
FV	7.51×10^{-18}	2.18	15.6	0.1
FR	7.04×10^{-11}	1.30	16.5	0.1
FP	2.01×10^{-28}	3.18	16.6	0.1
Nylon 6	2.07×10^{-19}	2.41	4.04	0.1

this indicated that ΔH was independent of the fiber orientation. Note that the values of A and n were affected by the fiber orientation. The properties listed in Table II were quite different from those of the TP sample (see Table I). This suggested that the creep properties of the fiber-reinforced nylon 6 material should be determined from actual products.

Stress relaxation

The relationships between the retention force and the time of the press-fit component (Fig. 2) for various temperature conditions are shown in Figure 9(a). In all cases, the retention force initially decreased with time and then reached an almost constant value. The initial retention force was 1.5 kN but decreased to a constant value of about 0.8 kN for 24 h at 343 K. On the other hand, the decrease in the retention force was more significant at higher temperatures, and the values of the retention force were about 0.4 and 0.2 kN for 24 h at 393 and 423 K, respectively. The temperature dependency of the retention force was interpreted as the stress relaxation of the fiber-reinforced nylon 6 product.

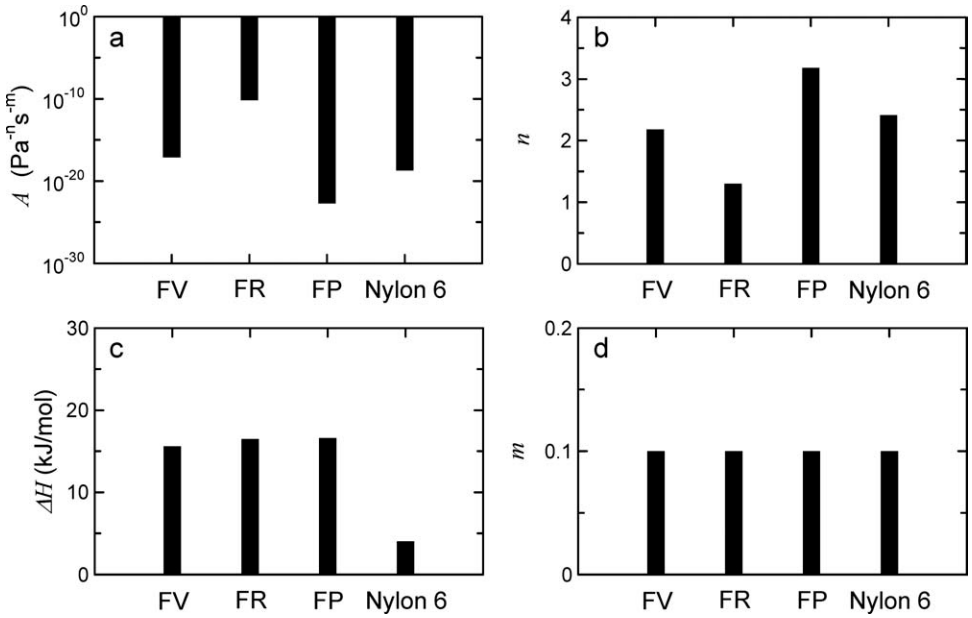

Figure 8 Creep properties of the various samples. (a) A, (b) n, (c) ΔH, and (d) m.

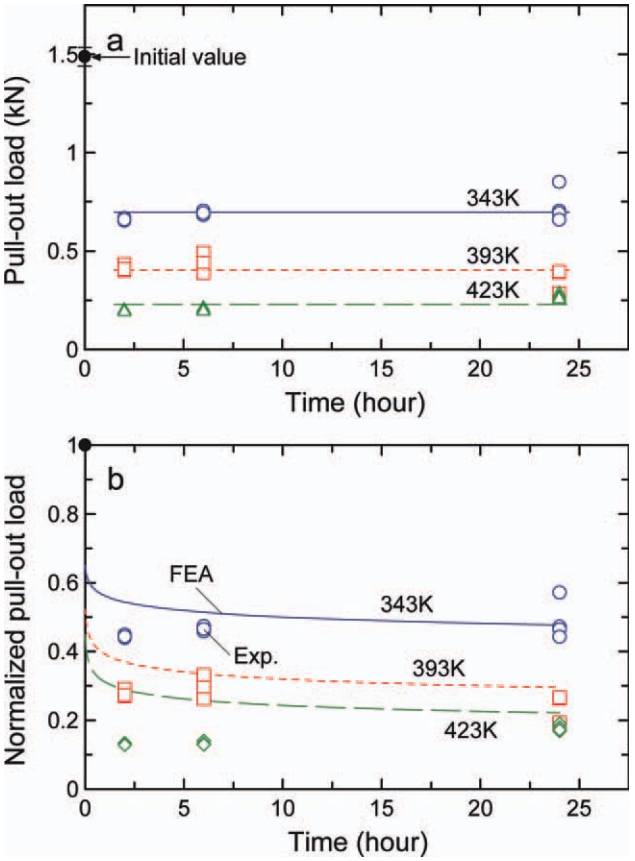

Figure 9 (a) Behavior of the retention force against time at various temperatures. (b) Comparison of the experimental (plot) and FEA (curve) results for the normalized retention force. [Color figure can be viewed in the online issue, which is available at wileyonlinelibrary.com.]

Figure 9(b) shows the normalized retention force at temperatures of 343, 393, and 423 K, obtained by FEA, together with the experimental ones. Here, the normalized retention force was defined as P/P_0, where P_0 is the initial value of the load. In FEA, the creep properties summarized in Table I were used to determine F. The value of E of the fiber-reinforced nylon 6 material was assumed to be the value at higher temperature if the resin had once been subjected to the higher temperature. It was reported that the value of E of a polymer is affected by the creep and recovery.[22] From the figure, the decrease in the normalized retention force against time at various temperatures obtained by FEA was in good agreement with the experimental results. This indicated that it is possible to predict the retention force by FEA. This also supports the validity of the method used here for determining the creep properties of a fiber-reinforced nylon 6 product.

Effect of the fiber orientation on the stress relaxation

Let us consider the effect of the fiber orientation on the stress relaxation of the press-fit component treated in the previous section. Figure 10(a–c) shows that the relationships between the normalized retention force and the time for the press-fit components composed of the metal collar and the artificial fiber-reinforced nylon 6 products with creep properties of the FV, FR, and FP samples. Three temperature conditions, 343, 393, and 423 K, were used. Although the model used for FEA was the same in all cases, the behavior of the normalized retention force for each artificial product was quite different. This indicated that the fiber direction in the nylon 6 materials against load highly affected the stress relaxation of the press-fit component. For example, the values of the normalized retention force of the FP product, which had the largest value of n in the examined beam samples, decreased dramatically in the early stages at all temperatures. In this case, the stress relaxation of the press-fit component was highly affected by stress rather than temperature.

Figure 11(a) shows the relationships between the normalized retention force after 24 h and the temperature. The difference in the normalized retention

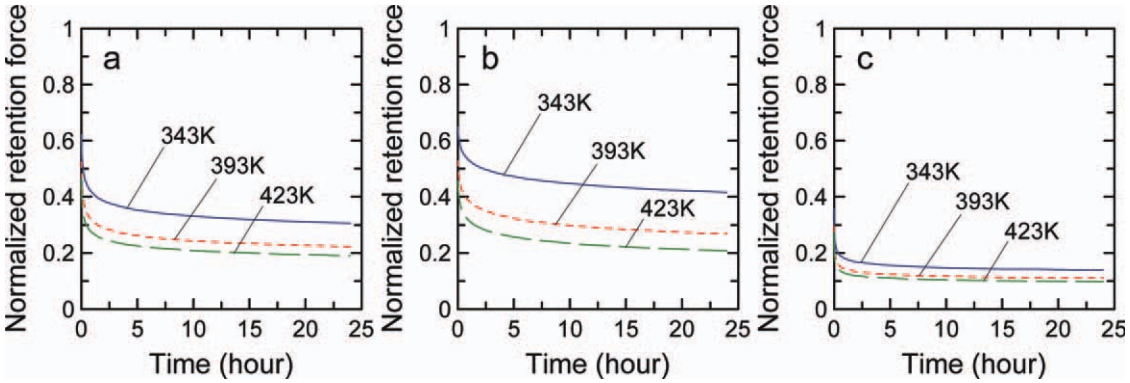

Figure 10 Behavior of the normalized retention force of artificial products predicted by FEA with the assumption of the creep properties of the (a) FV, (b) FR, and (C) FP samples. [Color figure can be viewed in the online issue, which is available at wileyonlinelibrary.com.]

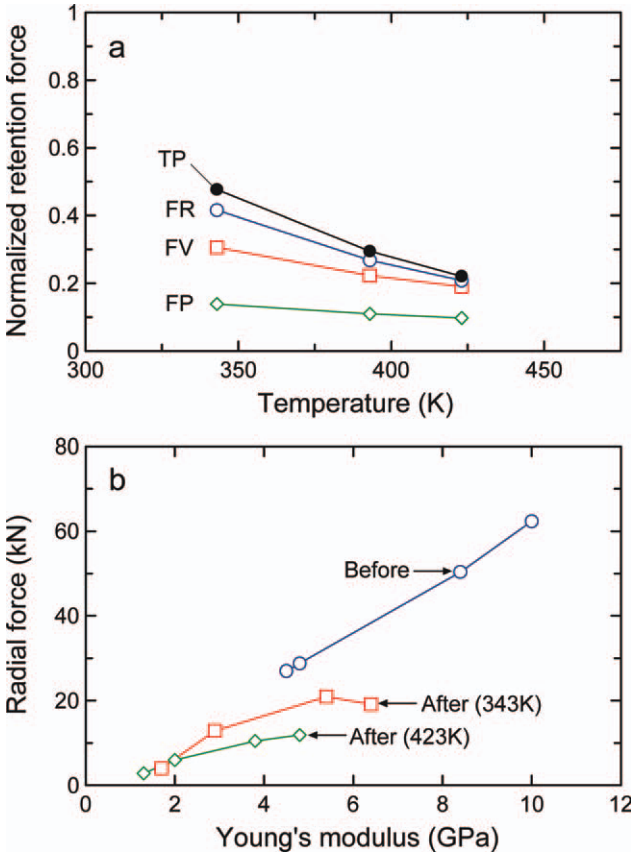

Figure 11 (a) Normalized retention force after 24 h versus temperature. (b) Relationship between F after 24 h and E. [Color figure can be viewed in the online issue, which is available at wileyonlinelibrary.com.]

force among the press-fit components was obvious at lower temperature. Figure 11(b) represents the relationship between F and E initially and after 24 h at 343 and 423 K. In the case of the press-fit components subjected to a temperature of 423 K, the fiber-reinforced nylon 6 product with the highest E gave the highest value of F in the products considered. On the other hand, for the components subjected to 343 K, the fiber-reinforced nylon 6 product with the second highest value of E gave the highest F in the considered products. The FEA results suggest that the higher stress field developed initially due to the higher value of E accelerated the stress relaxation of the press-fit component at 343 K. In other words, strong fiber-reinforced nylon 6 material is not always the best for enhancing the long-term reliability of press-fit components.

CONCLUSIONS

In summary, we proposed a technique to determine the creep properties of a fiber-reinforced nylon 6 product with the aid of FEA. The creep behavior of the cylindrical and beam samples made of the fiber-reinforced nylon 6 material were recorded by compression or three-point bending creep tests, and the creep properties of the fiber-reinforced nylon 6 materials with various fiber orientations were successfully determined by the fitting of analytical curves to the experimental data. Finally, the stress relaxation of the press-fit component composed of the fiber-reinforced nylon 6 product with a through-hole and metal collars was successfully analyzed by FEA, where the experimentally determined creep properties of the fiber-reinforced nylon 6 product were used. Note that the stronger fiber-reinforced nylon 6 material with higher E developed a higher stress field in the material, which could, therefore, sometimes accelerate the stress relaxation of the press-fit component.

The authors thank Prof. M. Saka for valuable discussions throughout this work, Prof. T. Yokobori for his helpful discussions, and also Mr. H. Suzuki and Ms. M. Miura for their help in the experiments.

APPENDIX

Temperature dependency of E

Figure A1 shows the relationships between the measured values of E and the temperature for the examined fiber-reinforced nylon 6 samples. The values of E for all of the samples showed a temperature dependency, and these decreased with increasing temperature. Because the glass-transition temperature of nylon 6 was 321 K, the values of E for the examined samples dramatically decreased in the range 293–343 K. Over the examined temperature range, the FV sample had the highest values of E, and these values were three times larger than those of the FP sample, which had the lowest E.

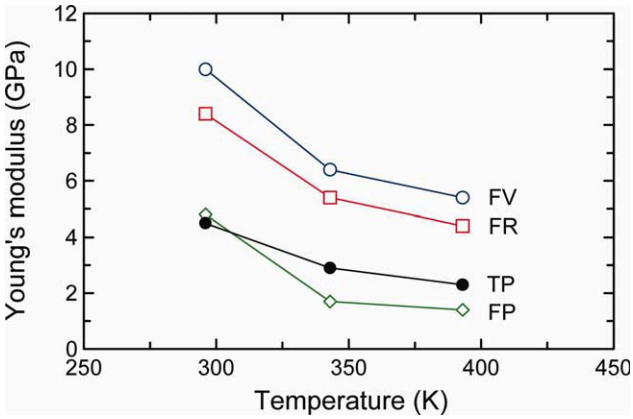

Figure A1 Relationships between E and temperature for fiber-reinforced nylon 6 samples. [Color figure can be viewed in the online issue, which is available at wileyonlinelibrary.com.]

References

1. Beardmore, P. Compos Struct 1986, 5, 163.
2. Soutis, C. Mater Sci Eng A 2005, 412, 171.
3. Li, J.; Weng. G. J. Compos B 1996, 27, 589.
4. Le Moal, P.; Perreux, D. Compos Sci Technol 1994, 51, 469.
5. Venkatesh, T. A.; Dunand, D. C. Acta Mater 1999, 47, 4275.
6. Beijer, J. G. J.; Spoormaker, J. L. Polymer 2000, 41, 5443.
7. Dean, D.; Husband, M.; Trimmer, M. J Polym Sci Part B: Polym Phys 1998, 70, 2971.
8. Vlasveld, D. P. N.; Bersee, H. E. N.; Picken, S. J. Polymer 2005, 46, 12539.
9. Hunt, D. G.; Darlington, M. W. Polymer 1979, 20, 241.
10. Habeger, C. C.; Coffin, D. W.; Hojjatie, B. J Polym Sci Part B: Polym Phys 2001, 39, 2048.
11. O'Connell, P. A.; Hutcheson, S. A.; Mckenna, G. B. J Polym Sci Part B: Polym Phys 2008, 46, 1952.
12. Marais, C.; Villoutreix, G. J Appl Polym Sci 1998, 69, 1983.
13. Jack, D. A.; Smith, D. E. Compos A 2007, 38, 975.
14. Kang, G.-Z.; Yang, C.; Zhang, J.-X. Compos A 2002, 33, 647.
15. Sala, G.; Landro, L. D. Polym Compos 1997, 18, 28.
16. Shimizu, M.; Adachi, T.; Arai, M.; Matsumoto, H. Trans JSME Ser A 1999, 65, 2060 (in Japanese).
17. Wang, H. W.; Zhou, H. W.; Peng, R. D.; Mishnaevsky, L., Jr. Compos Sci Technol 2011, 71, 980.
18. Ohno, N.; Wu, X.; Matsuda, T. Int J Mech Sci 2000, 42, 1519.
19. Hult, J. A. H. In Engineering Structures; Blaisdell: Waltham, MA, 1966.
20. MSC Software Corp. In Marc User's Guide; MSC: Santa Ana, CA, 2003.
21. Tohmyoh, H.; Yamanobe, K.; Saka, M.; Utsunomiya, J.; Nakamura, T.; Nakano, Y. J Electron Packag 2008, 130, 031007.
22. Rogozinsky, A. K.; Bazhenov, S. L. Polymer 1992, 33, 1391.